

This item is the archived peer-reviewed author-version of:

How flexibility and eardrum cone shape affect sound conduction in single-ossicle ears : a dynamic model study of the chicken middle ear


Reference:


Muyshondt Pieter, Dirckx Joris.- How flexibility and eardrum cone shape affect sound conduction in single-ossicle ears : a dynamic model study of the chicken middle ear
Biomechanics and modeling in mechanobiology - ISSN 1617-7959 - (2019), p. 1-17
Full text (Publisher's DOI): <https://doi.org/10.1007/S10237-019-01207-4>
To cite this reference: <https://hdl.handle.net/10067/1629620151162165141>

How flexibility and eardrum cone shape affect sound conduction in single-ossicle ears: a dynamic model study of the chicken middle ear

Pieter G.G. Muyshondt^{a,1}, Joris J.J. Dirckx^{a,2}

^a *University of Antwerp, Biophysics and Biomedical Physics, Groenenborgerlaan 171, 2020 Antwerp, Belgium*

5 ¹ *E-mail:* pieter.muyshondt@uantwerpen.be; *Phone:* +3232653438;  0000-0003-0636-1731

²  0000-0002-2664-1207

Abstract

It is believed that non-mammals have poor hearing at high frequencies because the sound-conduction performance of their single-ossicle middle ears declines above a certain frequency. To better understand this behavior, a dynamic three-dimensional finite-element model of the chicken middle ear was constructed. The effect of changing the flexibility of the cartilaginous extracolumella on middle-ear sound conduction was simulated from 0.125 to 8 kHz, and the influence of the outward-bulging cone shape of the eardrum was studied by altering the depth and orientation of the eardrum cone in the model. It was found that extracolumella flexibility increases the middle-ear pressure gain at low frequencies due to an enhancement of eardrum motion, but it decreases the pressure gain at high frequencies as the bony columella becomes more resistant to extracolumella movement. Similar to the inward-pointing cone shape of the mammalian eardrum, it was shown that the outward-pointing cone shape of the chicken eardrum enhances the middle-ear pressure gain compared to a flat eardrum shape. When the outward-pointing eardrum was replaced by an inward-pointing eardrum, the pressure gain decreased slightly over the entire frequency range. This decrease was assigned to an increase in bending behavior of the extracolumella and a reduction in piston-like columella motion in the model with an inward-pointing eardrum. Possibly, the single-ossicle middle ear of birds favors an outward-pointing eardrum over an inward-pointing one as it preserves a straight angle between the columella and extrastapedius and a right angle between the columella and suprastapedius, which provides the optimal transmission.

Keywords

25 Bird middle ear; Finite-element modeling; Sound conduction; Tympanic Membrane; (Extra)columella

Electronic supplementary material

The online version of this article (<https://doi.org/10.1007/s10237-019-01207-4>) contains supplementary material, which is available to authorized users.

1. Introduction

30 The middle ear (ME) is a complicated biomechanical system that contains an eardrum or tympanic membrane (TM) and one or more hearing bones, called ossicles. In mammals, the ME contains three ossicles, named the malleus, incus and stapes. In non-mammalian terrestrial vertebrates, the ME contains only a single ossicle, called the stapes or columella. Generally, it is thought that the ME of mammals and non-mammals developed independently from each other (Manley 2010). The function of the ME is to match the acoustic impedance of
35 sound waves in air and in the inner-ear (IE) fluid, which is mainly done through two mechanisms: (1) an increase in the sound pressure by projecting the sound input at the large TM area onto the smaller area of the stapes footplate, and (2) a lever action of the ossicles which amplifies the force over the ossicular chain. It is believed that such a lever action is present in both the three-ossicle chain of mammals and the single-ossicle chain of non-mammals (e.g., Manley and Sienknecht 2013).

40 In amphibians, birds and many reptiles, the columella is connected to the TM by a flexible cartilaginous unit, called the extracolumella. In birds, crocodiles and some types of lizards, the extracolumella functions as a second-class lever (like a wheelbarrow) which is typically composed of two or three processes, although the design varies greatly among species (e.g., Mason and Farr 2013). The process that is mostly responsible for the conduction of sound from the TM to the IE is called the infrastapedius in lizards and extrastapedius in birds. It
45 pushes on the TM near the center of the membrane at a point denoted as the umbo. This connection typically gives the TM in non-mammals a curved, outward conical shape, which is opposite to the inward conical shape of the TM in mammals. In mammals, it has been shown that having a curved, inward conical TM enhances ME sound conduction (Funnell and Laszlo 1978; Funnell 1983; Koike et al. 2001; Fay et al. 2006). It is unclear whether the sound conduction in the single-ossicle ME of non-mammals benefits from the outward nature of the
50 curved, conical TM.

Although absolute minimum hearing thresholds in non-mammals are generally not inferior to the thresholds found in mammals, considerable differences exist in the frequency range of hearing. While terrestrial mammals can typically hear sounds up to several tens of kHz (20 kHz for humans up to over 100 kHz for mice), the auditory range of non-mammals never exceeds 10 kHz (Manley 1972a). This distinction in hearing ability can be
55 partially attributed to a difference in sensitivity of the IE sensory organ; when sound conduction through the ME is disregarded, the IE of non-mammals is increasingly poor in analyzing frequencies above about 5 kHz (Manley 1972a). However, as air-conducted sound must first pass through the ME to reach the IE, hearing ability also

depends on the sound-conduction performance of the ME. In fact, it is believed that the design of the single-ossicle ME in non-mammals constrains hearing at high frequencies (Manley 1972a).

60 This work investigates the mechanics of sound conduction in the single-ossicle ME by means of finite-element (FE) modeling. A linear dynamic three-dimensional (3D) FE model is developed, which is largely based on a previous nonlinear static FE model of the chicken ME (Muyschondt et al. 2019). The frequency response of the ME is simulated under sound-pressure stimulation of the TM. The chicken serves as model species for non-mammals with a ME that contains a TM, a single ossicle and an extracolumella that functions as a second-class
65 lever. First, the linear frequency response of the ME is validated against measurements of the ME vibration response to sound. Next, the model is used to study the effect of controlled changes in ME flexibility and TM cone shape on ME sound conduction.

2. Materials and methods

2.1 *Finite-element model*

70 2.1.1 *Model geometry*

The model used in the current paper is based on a 3D FE model that was previously developed to study the nonlinear static deformation behavior of the chicken ME under large static pressures (Muyschondt et al. 2019). The geometry of the model was extracted from a micro-CT scan of the left ear of a female domestic chicken. The reconstructed scan had a voxel size of 10.9 μm . Semi-automatic image segmentation was performed in Amira
75 6.3 (FEI, Hillsboro, OR, USA) to identify the ME components. The segmented data set was converted into a triangulated surface model, which is shown in Fig. 1 with all components indicated. The three processes of the extracolumella, called the infra-, extra- and suprastapedius, are denoted. Beside the TM, columella and extracolumella, the model also includes the ascending ligament, infrastapedial membrane and Platner's ligament. For more details on the micro-CT scanning, image segmentation and geometrical model, the reader is referred to
80 Muyschondt et al. (2019). The ear canal, ME cavity and fluid-filled IE were not included in the model.

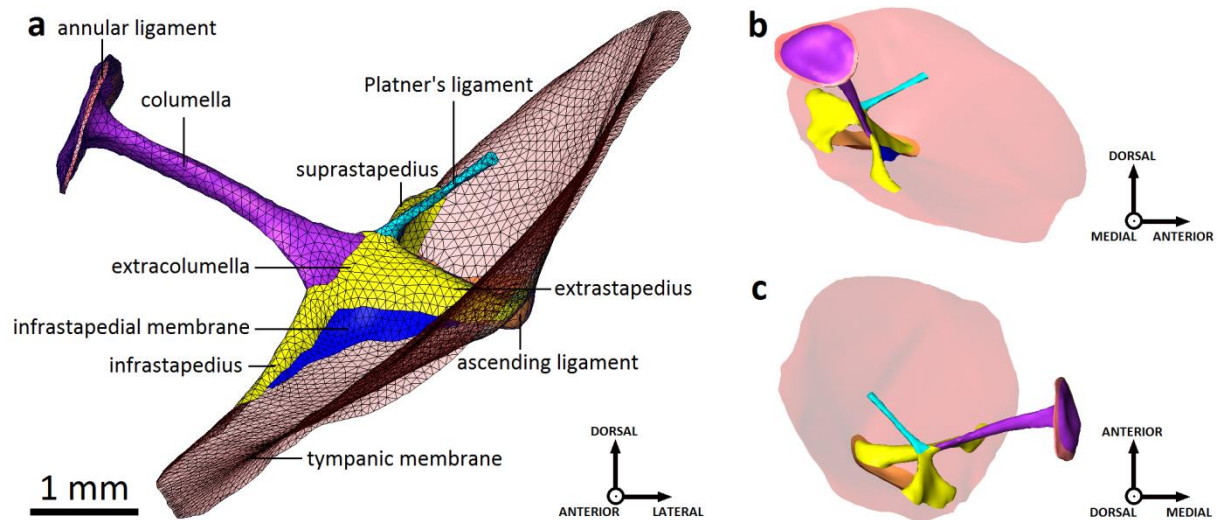


Fig. 1 Triangulated surface model of the left ME of a female chicken used as geometry for the FE model (**a** anterior view; **b** medial view; **c** dorsal view). The different ME components are indicated, and the TM was made partially transparent to better visualize the underlying structures

85 2.1.2 Model description

The geometrical surface model of the ME was imported as an STL file into the commercial FE software COMSOL, version 5.3a (COMSOL Multiphysics, Burlington, MA, USA). Instead of using solid elements for all structures as in the previous version of the FE model, the present model used triangular shell elements for the TM and tetrahedral solid elements for all other structures. The order of the elements was quadratic. Solid and shell objects shared translational and rotational degrees of freedom at their connections. The thickness distribution of the TM was extracted from the micro-CT data and was applied to the TM shell surface. The thickness map was obtained by calculating the point-wise shortest distance between the upper and lower surface of the segmented TM, based on the method of Van der Jeught et al. (2013). Figure 2 shows the TM thickness map after smoothing out irregularities. The thickness of the ascending ligament was not incorporated in the TM thickness map. The vertical line of increased thickness between the tip of the ascending ligament and the anteroventral rim of the TM (Fig. 2) corresponds to the middle drum-tubal ligament (Pohlman 1921), which was not modeled as a separate component but included in the TM thickness instead. Also the intracolumellar connection, that is, the junction zone between the columella and extracolumella, was not simulated as a separate structure; although it was identified as a zone of flexibility (Smith 1904; Pohlman 1921; Norberg 1978; Starck 1995; Mills and Zhang 2006; Arechvo et al. 2013), it is not a joint but a transition zone between cartilage and bone (Arechvo et al. 2013). In the model, the connection was considered as an abrupt transition from cartilage to bone. Similar to the situation in mammals, the TM in chicken is not directly surrounded by a bony ring (Pohlman

1921), but transitions into a thick border of soft tissue before it connects to the surrounding bone. This soft support possibly increases the freedom of movement of the TM boundary, so the periphery of the TM was simulated as simply supported instead of fully clamped. Changing the TM boundary to fully clamped decreased the footplate response by only 0.5 dB below the first resonance and had almost no effect above the first resonance (not shown). The ME muscle, which is attached to the posteromedial rim of the TM, was considered to have a merely passive effect. Hence, this part of the TM rim was simulated using the same boundary condition as other parts of the TM periphery, and the ME muscle was disregarded. The boundary elements that form the periphery of the annular ligament and the distal end of Platner's ligament were modeled as fixed.

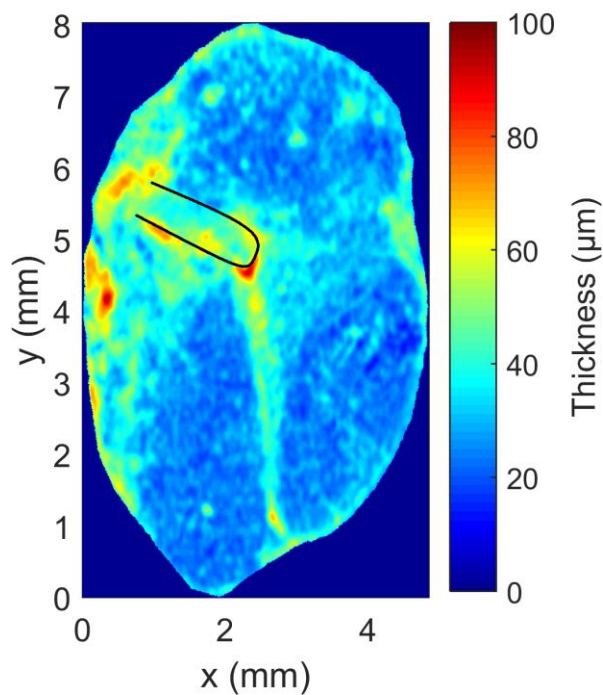


Fig. 2 Thickness distribution of the TM in chicken, calculated from the segmentation of the micro-CT scan (dorsomedial view). The attachment location of the ascending ligament is indicated by a black line

2.1.3 The inner-ear load

The IE was not included as a separate part in the FE model. Instead, the load of the IE was simulated as a uniform pressure $P_{IE} = Z \cdot U$ normal to the medial footplate surface. In this expression, Z represents the acoustic input impedance of the IE and U is the combined volume velocity of the columellar footplate and annular ligament in the oval window. The acoustic impedance has the form $Z = R + i\omega M$, with R the *acoustic* resistance, M the *acoustic* mass, ω the angular frequency and i the imaginary unit. Z did not include an acoustic stiffness, as it was shown in ostrich that the avian IE load has no important effect on quasi-static footplate displacements

(Muysshondt et al. 2016), which is mainly controlled by stiffness. R and M were estimated by geometrically scaling the experimentally determined values of R and M in ostrich (Muysshondt et al. 2016) to chicken. In mammals, the *specific* acoustic input impedance of the IE z is mainly dominated by resistance and independent of animal size (Hemilä et al. 1995). The relation between the characteristic acoustic impedance Z and specific acoustic impedance z is $Z = z/A$, with A the surface area of the footplate. Extrapolating the findings of Hemilä et al. (1995) from mammals to birds, the IE acoustic resistance R was scaled from ostrich to chicken using $R_C = R_O \cdot (A_O/A_C)$ (C: chicken; O: ostrich). For the mass component, the relation between *acoustic* mass M and *mechanical* mass m is $M = m/A^2$, with A the surface area of the footplate. If it is assumed that the mechanical mass of the IE load m is proportional to the IE volume V , and that this relation is the same in ostrich and chicken, the scaling of *acoustic* mass M from ostrich to chicken becomes $M_C = M_O \cdot (V_C/V_O) \cdot (A_O/A_C)^2$. IE volumes V_C & V_O and footplate surface areas A_C & A_O were obtained from micro-CT data. The estimated parameter values of the IE load in chicken were $R_C = 3.34 \times 10^9$ Pa s/m³ and $M_C = 0.686 \times 10^6$ Pa s²/m³.

2.1.4 Sound-pressure stimulation

The frequency of the harmonic input pressure in the model ranged from 0.125 to 8 kHz, using a spacing of 8 lines per octave. This frequency range largely covered the auditory range of the chicken, which ranges from 9.1 Hz to 7.2 kHz (Hill et al. 2014). Chickens are thus sensitive to infrasound, but as the ME behavior doesn't change below the first resonance frequency, there was no need to evaluate the response down to 9.1 Hz. The upper bound of 8 kHz was high enough to capture the decreasing performance of the single-ossicle ME at high frequencies.

The ear canal was not included in the model. Instead, the sound pressure of the incoming sound wave was directly applied to the lateral TM surface as a harmonic pressure load with uniform amplitude (1 Pa) and phase (0°). The assumption of sound-pressure uniformity is quite consistent with measurements of the sound-pressure distribution over the TM surface in, e.g., gerbil (Bergevin and Olson 2014). As the ear canal in chicken is quite short (~ 9 mm), it does not provide a meaningful sound-pressure amplification at the TM through resonance; considering that the ear canal is an open-closed cavity, the first standing mode will occur at about 9.5 kHz, which is above the upper audible frequency in chicken and the maximal frequency investigated here (8 kHz). A standing mode at 9.5 kHz might have a small effect at the highest frequencies up to 8 kHz, but the effect will be the same for all models investigated our study. Because our focus is on comparing the outcome of the different models, the conclusions of our work would remain.

150 The impedance of the air in the ME cavity was also not included in the model. The radiance of the cavity (real part of the impedance) was estimated by Maftoon et al. (2015) in gerbil and was found to be much smaller than that of the ME components and cochlea. By doing the same estimation for the chicken (Kinsler et al. 1999, p. 186), the calculated radiance of the ME cavity was found to be more than four orders of magnitude smaller than the estimated IE acoustic resistance R , so it was excluded. As the cavity is closed under normal
155 circumstances, it could act as a compliance. However, the compliance was disregarded as the model is compared to measurements with an opened cavity (see Sect. 3). In a closed ME cavity, the compliance of the enclosed air is proportional to the volume of the cavity (e.g., Motallebzadeh et al. 2017). In birds, the ME cavities are internally connected through a large air space in the skull (e.g., Larsen et al. 2016) whose volume is much larger than the volume displacement of the TM. Therefore, the effect of the cavity compliance in birds will be much smaller
160 than for the isolated ME cavities in mammals. The mass load of the air in the cavity was neglected, as was done in, e.g., Motallebzadeh et al. (2017).

2.1.5 *Material properties*

All ME structures were modeled using constant, homogeneous, isotropic material parameters. Table 1 lists the material parameter values of the model components, including the elastic Young's moduli E , Poisson's ratios ν ,
165 mass densities ρ and damping loss factors η . In mammals, the TM is often modeled as a radial orthotropic elastic material to simulate the arrangement of radial and circumferential collagenous fibers in the TM. In chickens, the TM contains radial and non-radial fibers, but the non-radial fibers have a complicated distribution and orientation (Filogamo 1949). The radial orthotropic description in mammals would therefore not be appropriate in chicken. In a human ME model, the footplate vibration response within the auditory frequency range was
170 affected by less than 3.3 dB when changing the isotropic elastic description of the TM by an orthotropic one (De Greef et al. 2017). For this reason and for the sake of simplicity, an isotropic characterization was used for TM elasticity in the present model. The values of the soft-tissue Young's moduli in the present dynamic model were not the same as in our previous static model (Muyschondt et al. 2019); the reason is that the dynamic stiffness of viscoelastic materials can change with frequency, thus differing from the (quasi-)static stiffness. The real part of
175 the dynamic modulus (i.e., the storage or elastic modulus) of the TM, ossicular joints and annular ligament in human was shown to increase with frequency due to viscoelasticity (Zhang and Gan 2013, 2014; Jiang and Gan 2018). To incorporate this increased stiffness effect in the present dynamic model, the Young's moduli of the soft-tissue structures in the static model were multiplied by a constant factor. A multiplication factor of 2 for all soft tissues was selected by trial and error, which resulted in a good correspondence with measurements of the

180 ME response in chicken. This factor was of the same order as the increase of the dynamic moduli relative to the
 (quasi-)static moduli found in human (Zhang and Gan 2013, 2014; Jiang and Gan 2018). The imaginary part of
 the dynamic modulus (i.e., the loss modulus) describes the viscous losses in a viscoelastic material. Losses were
 modeled by using a constant damping loss factor; a value of 0.3 for all soft tissues resulted in a good
 185 resemblance to experimental data (see Sect. 3). The remaining Young's moduli, Poisson's ratios and mass
 densities were based on frequently used values for soft tissue and bone in ME models (Gan et al. 2004; Kirikae
 1960; Maftoon et al. 2015).

Table 1 Material parameter values used in the FE model. E Young's modulus; ρ mass density; ν Poisson's ratio; η damping
 loss factor. The Young's moduli of the soft-tissue components in the dynamic model were obtained by doubling the values of
 the Young's moduli in our previous static model (Muyshondt et al. 2019). The damping loss factors were manually adjusted
 190 to obtain a good resemblance to experimental data. ^a Gan et al. (2004), ^b Kirikae (1960), ^c Maftoon et al. (2015)

Component	E (MPa)	ρ (10^3 kg/m ³)	ν	η
Columella	14100 ^a	2.2 ^b	0.3 ^c	0
Annular ligament	0.1	1.1 ^c	0.49 ^c	0.3
Tympanic membrane	2	1.1 ^c	0.49 ^c	0.3
Infrastapedial membrane	2	1.1 ^c	0.49 ^c	0.3
Ascending ligament	6	1.1 ^c	0.49 ^c	0.3
Extracolumella	6	1.1 ^c	0.49 ^c	0.3
Platner's ligament	42	1.1 ^c	0.49 ^c	0.3

2.1.6 Sensitivity analysis

As a priori knowledge of material parameters in the chicken ME is lacking, there is considerable uncertainty in
 the parameter values in Table 1. To investigate the sensitivity of the model to these parameters, models with a
 low and high ME impedance were evaluated in addition to the base model in the examined frequency range. In
 195 these models, the Young's moduli, mass densities and damping loss factors were, simultaneously, decreased and
 increased by 50%, respectively. To determine the effect of the IE load, models with a low and high IE
 impedance were evaluated, in which the IE load was decreased and increased by 50%, respectively. To
 determine the effect of each parameter individually, the ME parameters (Table 1) and IE parameters (R and M)
 were consecutively decreased and increased by 50% while keeping all other parameters at their base value, and
 200 the model was evaluated at 0.125, 1 and 8 kHz. Applying 50% variations to all parameters neglects the fact that
 the uncertainty is greater for some parameters than others, but it allows us to compare the intrinsic effects of all
 parameters. The mass density ρ , Poisson's ratio ν and loss factor η of the soft-tissue structures were regarded as
 shared parameters for all soft tissues combined (ρ_{st} , ν_{st} , η_{st}), so each parameter was varied for all soft tissues at

once. The soft-tissue Poisson's ratio was only decreased and not increased by 50%, because it cannot exceed a value of 0.5. To investigate the effect of decreased flexibility on sound conduction in the single-ossicle ME, the elasticity of the columellar apparatus was artificially increased. The flexibility of the columellar apparatus is typically associated with the cartilaginous extracolumella. To simulate a completely ossified columellar apparatus, the Young's modulus of the extracolumella ($E = 6$ MPa) was increased to equal the Young's modulus of the bony columella ($E = 14.1$ GPa).

2.1.7 Shape of the tympanic-membrane cone

To investigate the effect of the orientation and depth of the TM cone, four models with modified ME geometry were created in addition to the normal geometry (Fig. 3a). In the first model, the outward TM cone was made flat (Fig. 3b); in the second model, the outward TM cone was inverted to form a TM cone with inward TM cone (Fig. 3c); in the third model, the depth of the outward TM cone was decreased by 50% to form a shallow TM (Fig. 3d); in the fourth model, the depth of the outward TM cone was increased by 50% to form a deep TM (Fig. 3e). The procedure to create the modified geometries was the same as in our previous static model, which is explained in Muyschondt et al. (2019). In this procedure, the angle of the columellar shaft relative to the TM base plane was preserved. Due to this restriction, the extracolumella was deformed such that the inclination of the extrastapedius relative to the columellar shaft was changed, and the configuration of the infra- and suprastapedius was altered. This can be seen in the different geometries, especially with inverted TM (Fig. 3c).

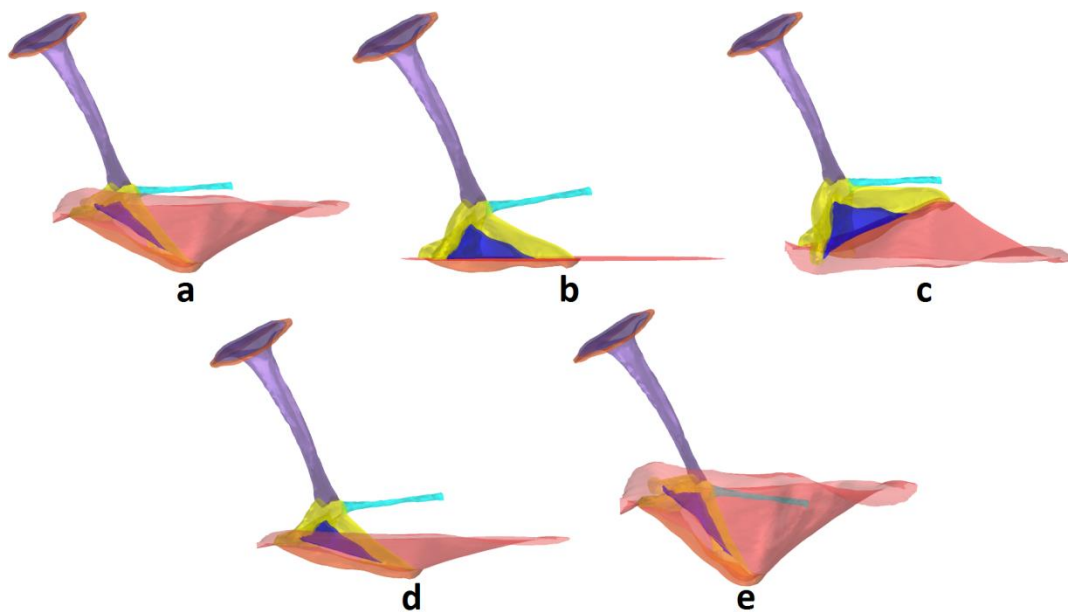


Fig. 3 Original and modified ME geometries of the chicken ME model (anteroventral view). The figure shows the normal ME geometry with **a** an outward TM cone, and modified ME geometries with **b** a flat TM, **c** an inverted inward TM cone, **d** a TM cone with the original depth reduced by 50%, and **e** a TM cone with the original depth increased by 50%

225 2.1.8 *Computational specifications*

Computations were executed on a personal computer (Intel(R) Xeon(R) CPU E5-2630 v3, 2.40 GHz (2 processors), and 128 GB of RAM). A convergence analysis was done to determine the appropriate mesh size of the model that resulted in a good compromise between model accuracy and computational time. The relative difference of the footplate vibration level between the second-to-finest mesh (156,588 number of DOFs) and the
230 finest mesh (209,967 number of DOFs) was less than 1 dB in the investigated frequency range. The model with the finest mesh was used for the simulations. The computation of the base model took 1 h 42 min.

3. Results

3.1 *Model validation*

Before the model was used to investigate the effect of ME flexibility and TM cone orientation, it was validated
235 against measurements of the footplate vibration response in chicken. Figure 4 compares the magnitude and phase of the footplate piston velocity response in the model with four ex vivo measurements in chicken. The phase was only available for two measurements. The experimental curves were obtained by 1D laser Doppler vibrometry measurements on the medial surface of the footplate after the intracranial air space was opened and the IE was destroyed and drained. The laser beam was approximately perpendicular to the plane of the footplate and
240 positioned in the center of the footplate. Sound pressures were introduced and measured at the entrance of the sealed ear canal.

The base model and the models with low and high ME impedance were first calculated without an IE load applied to the footplate, similarly to the measurements. The velocity magnitude in the model with low ME impedance is too large at low and mid frequencies, and the resonance peak and the large fluctuations at mid and
245 high frequencies are more pronounced than in the measurements. The velocity magnitude in the model with high ME impedance, on the other hand, is too small at low and high frequencies. The base model delivers a good compromise between the two extreme conditions, as it shows a reasonable agreement with the measurements in the investigated frequency range. The agreement is less good at high frequencies and in the phase, and there is a substantial amount of variability between the measurements, especially at high frequencies. When the IE load is
250 added to the model, the velocity magnitude decreases by up to 10 dB for frequencies beyond the resonance peak. In the analyses that follow, the IE load is always included in the model.

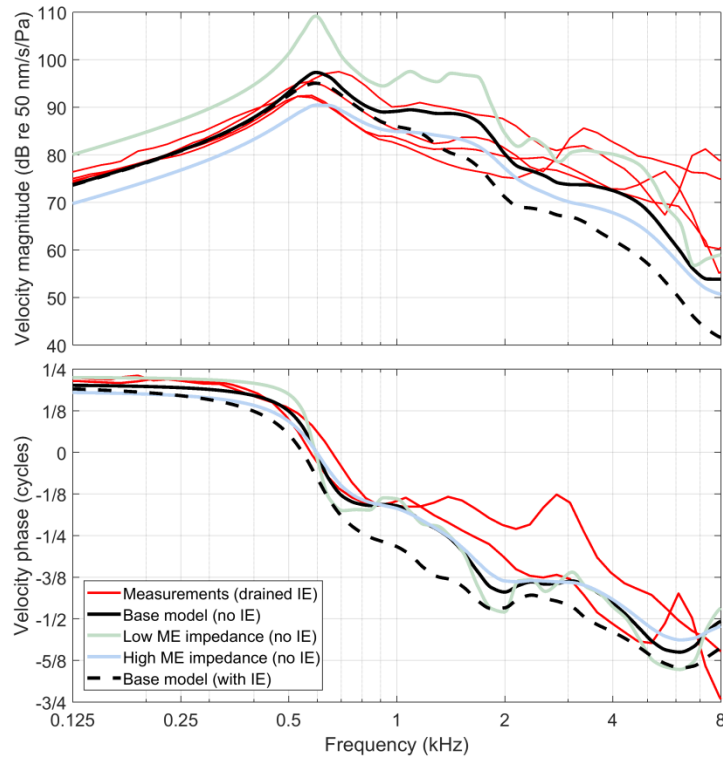


Fig. 4 Comparison of the measured and simulated footplate response in chicken. The low- and high-impedance models were obtained after respectively decreasing and increasing the base values of E , ρ and η together in Table 1 by 50%. The effect of including the IE load on the footplate response is shown

3.2 Sensitivity analysis

To examine the pressure-amplification performance of the ME, the pressure-gain function of the ME was evaluated. The ME pressure gain is defined as the ratio of the pressure output at the oval window to the pressure input at the TM. The output pressure is determined by the pressure load of the IE (P_{IE}), and the input pressure is equal to 1 Pa. Therefore, the pressure gain in the model is given by the value of P_{IE} . Figure 5 shows the simulated pressure gain of the ME for the base model and for the models with low and high ME and IE impedances. Similarly to the footplate response, the pressure-gain amplitude peaks around 0.6 kHz, but above this frequency, the amplitude decreases at a rate of about 10 dB/octave. Both for the ME and IE impedance, decreasing or increasing the material parameters of the base model mainly affects the gain amplitude at low and mid frequencies, the sharpness of the main peak and the degree of fluctuations in the pressure-gain function. The effect is opposite for the ME and IE impedances: the pressure gain decreases with increasing ME impedance, but increases with increasing IE impedance.

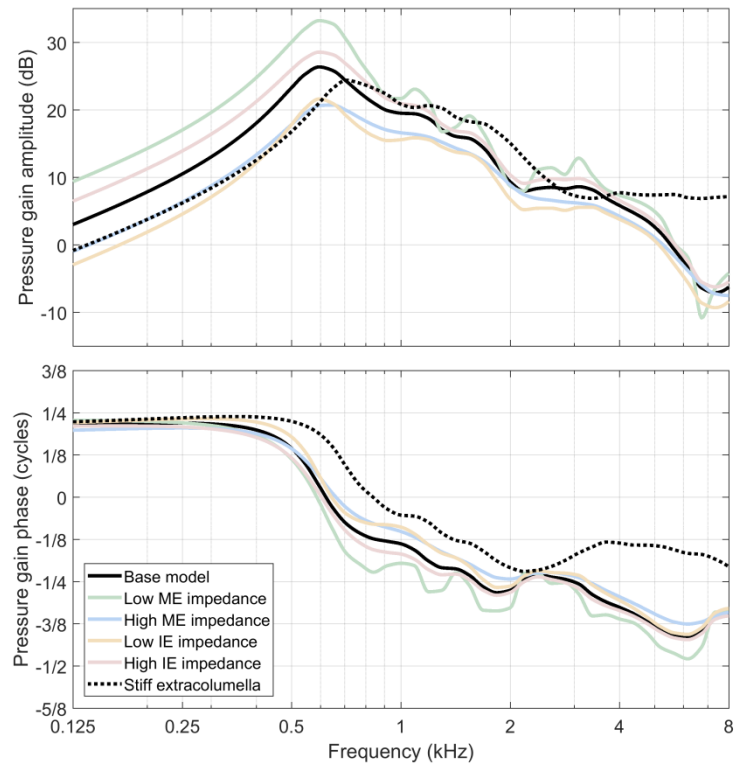
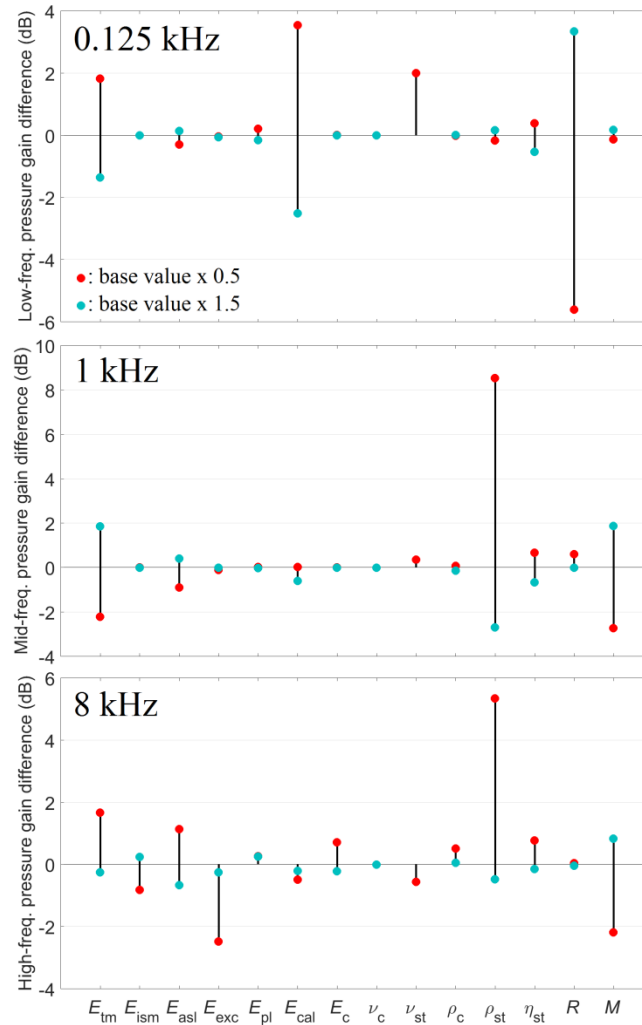


Fig. 5 Simulated pressure gain of the chicken ME for the base model, the models with low and high ME impedance, the models with low and high IE impedance and the model with stiff extracolumella

Figure 6 shows the sensitivity of the ME pressure gain amplitude to individual changes in the ME and IE parameters at 0.125, 1 and 8 kHz. At low frequencies, the pressure gain is mostly affected by (in decreasing order of magnitude) the IE acoustic resistance, the Young's moduli of the TM and annular ligament, and the soft-tissue Poisson's ratio. The effect is opposite for the mass densities and Young's moduli, except for the ascending ligament Young's modulus. At 1 kHz, the main effect comes from (in decreasing order of importance) the soft-tissue density, IE acoustic mass and TM Young's modulus. Although the effect of the soft-tissue density is large, the parameter is well established in ME research with little uncertainty in the base value. At high frequencies, the effect is also largest for the soft-tissue density, followed by (in decreasing order of magnitude) the IE acoustic mass and the Young's moduli of the extracolumella, TM and ascending ligament. For some parameters, an increase or decrease causes a change in the same direction (E_{exc} , E_{pl} , E_{cal} , ρ_c), which shows that the relation between the parameters and the ME response is not monotonic at high frequencies, so it is more complicated than at low and mid frequencies.



285 **Fig. 6** Changes in ME pressure gain amplitude at a low frequency (0.125 kHz), mid frequency (1 kHz) and high frequency (8 kHz) as the ME and IE parameters were varied (red: 50% decrease, green: 50% increase). ν_{st} was only decreased by 50%. When red dots are not visible, they are overlapping with green dots. E Young's modulus, ρ mass density, η loss factor, R IE acoustic resistance, M IE acoustic mass, ν Poisson's ratio, tm tympanic membrane, ism infrastapedial membrane, asl ascending ligament, exc extracolumella, pl Platner's ligament, cal columellar annular ligament, c columella, st soft tissues

3.3 Flexibility of the single-ossicle ear

290 This section examines the effect of flexibility in the single-ossicle ear on the sound-conduction performance of the ME. Figure 5 compares the ME pressure gain in the model with flexible extracolumella ($E = 6$ MPa) to the model with stiff extracolumella ($E = 14.1$ GPa). Increasing the stiffness of the extracolumella decreases the low-frequency gain amplitude by 4 dB and increases the main resonance frequency from 0.6 to 0.7 kHz. At frequencies above 3 kHz, the stiff model shows gain amplitudes that remain largely flat. As indicated by the high sensitivity to this parameter at 8 kHz (Fig. 6, lower panel), the gain of the stiff model deviates considerably from the flexible model at high frequencies.

To better understand the pressure-amplification behavior in Fig. 5, it is helpful to look at the vibration behavior of the single-ossicle ME. Figure 7 shows the deformations and displacements of the columellar apparatus in the flexible and stiff model at 0.125, 1 and 8 kHz. The deformed conditions in Fig. 7 are shown relative to the resting condition at the moment when the footplate is at its most inward position during a vibration period. The depicted displacements correspond to the root mean square (RMS) of the displacement vector magnitude. The motions of the columellar apparatus are also provided as video files (AVI) in the Supplementary material, which can help to better interpret the motion characteristics described in this section.

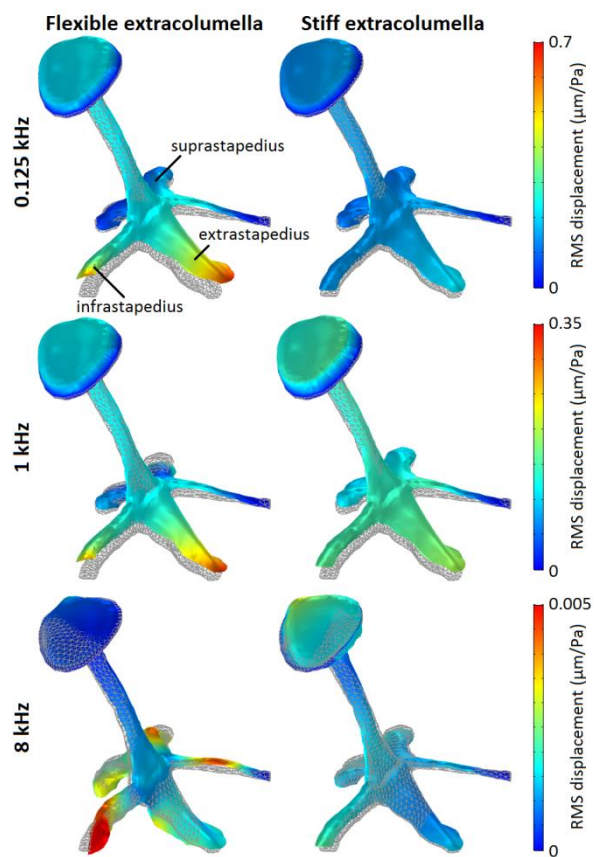


Fig. 7 RMS of the displacement vector magnitude of the columellar apparatus during stimulation at 0.125, 1 and 8 kHz (anteromedial view). The TM, ascending ligament and infrastapedial membrane are hidden. The deformed conditions (colored) are shown relative to the resting condition (triangulated) at the moment when the footplate is at its most inward position during a vibration period. The deformation is magnified by factors of 500, 1000 and 50,000 at 0.125, 1 and 8 kHz, respectively

At 0.125 kHz (Fig. 7, upper panels), the movement of the columellar apparatus is relatively uncomplicated. In the flexible model (left panel; Online Resource 1), the extracolumella mainly rotates around a fulcrum axis formed by the posterior edge of the TM at the distal end of the suprastapedius. This rotation is converted into a mainly piston-like motion of the columella and footplate, which is permitted by bending of the extrastapedius

over its entire length. The largest bending occurs at the point where the three processes of the extracolumella join together. The umbo and footplate vibrate in phase and show an amplitude ratio of 2.7. In the stiff model (right panel; Online Resource 2), the extracolumella more resembles a piston translation than a rotation; in fact, the rotation occurs around an axis located much farther away from the edge of the TM, so it looks more like a piston translation. The extracolumella transmits the piston-like motion from the umbo to the columella and footplate without any conversion by bending and with little reduction in magnitude from umbo to footplate. The amplitude ratio between umbo and footplate amounts to 1.5, without any phase lag in the vibration. Although the relative transfer of displacement from umbo to footplate is larger in the stiff model, it can be observed that the absolute “output” displacement at the footplate is larger in the flexible model. This is the case because the “input” displacement at the umbo is much larger in the flexible model than in the stiff model. This difference explains the superior pressure gain of the flexible model at low frequencies (Fig. 7).

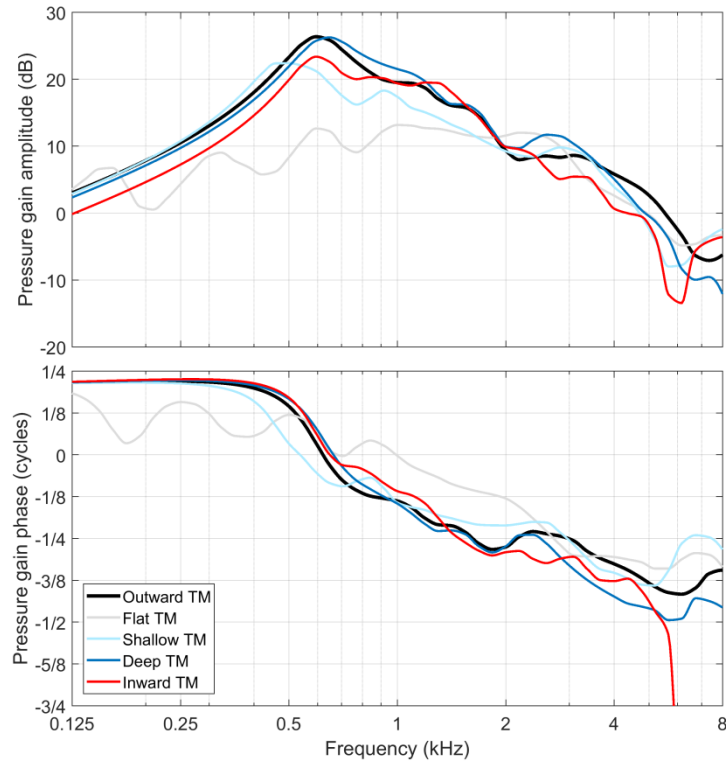
At 1 kHz (Fig. 7, middle panels), the columellar apparatus starts to become somewhat more complicated. In the flexible model (left panel; Online Resource 3), the rotation of the extracolumella around the posterior edge of the TM becomes less prominent. Another rotation arises around the long axis of Platner’s ligament, which can be observed by the fact that the suprastapedius moves in a direction opposite to that of the infra- and extrastapedius. This rotation is converted into a piston-like motion of the columella and footplate due to bending in the processes of the extracolumella. The columellar apparatus still shows a similar umbo-to-footplate ratio, although the umbo and footplate no longer vibrate exactly in phase. In the stiff model (right panel; Online Resource 4), the vibration behavior is similar to the motion seen at 0.125 kHz; the extracolumella mainly shows a piston translation that is largely transmitted to the columella and footplate without any conversion by bending, and the umbo and footplate still vibrate in phase. The umbo displacement is largest in the flexible model; however, the footplate displacement is largest in the stiff model. Therefore, the stiff model not only provides a better relative transfer of displacement from umbo to footplate than the flexible model, but also a better absolute transfer.

At 8 kHz (Fig. 7, lower panels), the motion behavior is much more complicated. In the flexible model (left panel; Online Resource 5), the extracolumella shows complicated bending patterns, where umbo displacements are guided to the columella as transverse traveling waves through the processes of the extracolumella. These motions are transmitted little beyond the point where the three processes of the extracolumella meet, which can be observed by the smaller displacement values of the extracolumella in this zone. As a result, the amplitude ratio between umbo and footplate increases markedly; i.e., the stiffness of the columella constrains the motion of the flexible extracolumella. The columella footplate does not display a pure piston-like motion but shows largely

rocking motions and small in-plane movements. In the stiff model (right panel; Online Resource 6), the
345 extracolumella performs a complicated translational and rotational type of motion which is strongly coupled to
the motion of the columella; in fact, the columella and extracolumella vibrate as one combined structure, and the
combined long axis of the columella and extrastapedius shows some bending. The footplate shows piston-like,
rocking and in-plane motions. Overall, the transfer of displacement from umbo to footplate is larger in the stiff
model than in the flexible model; although displacements of the extracolumella are largest in the flexible model,
350 they are better transmitted to the footplate in the stiff model. This difference in transmission largely explains the
superior pressure gain of the stiff model at high frequencies (Fig. 5).

3.4 *Orientation and depth of the tympanic-membrane cone*

This section investigates the effect of TM cone orientation and depth on the sound-conduction performance of
the single-ossicle ME. Figure 8 shows the pressure-gain function of the MEs with the different TM cone shapes.
355 When going from the normal outward model to the flat model, it is observed that the gain amplitude becomes
significantly smaller between 0.15 and 2 kHz, with reductions of up to 15 dB. The main resonance peak at 0.6
kHz vanishes, and local fluctuations arise below 2 kHz. Above 2 kHz, the pressure gains of the flat and outward
model are more alike, with differences of less than 4 dB. When switching from the normal model to the shallow
model, it can be seen that the main resonance frequency decreases from 0.6 to 0.45 kHz. Below 0.5 kHz, the gain
360 amplitude doesn't change considerably, with a minute increase of less than 2 dB. Between 0.5 and 2 kHz, the
gain amplitude decreases markedly by as much as 7 dB. Above 4 kHz, the gain amplitude mainly decreases by
up to 7 dB, with the exception of an increase beyond 6 kHz. When going from the normal model to the deep
model, it is observed that the main resonance frequency increases slightly from 0.6 to 0.65 kHz. Below 0.65
kHz, the gain amplitude remains similar, showing a minute decrease of less than 1.5 dB. Between 0.65 and 4
365 kHz, the gain amplitude increases by as much as 3 dB. Above 4 kHz, the gain amplitude diminishes by as much
as 6 dB. When the outward model is replaced by the inward model, it can be seen that the pressure gain
decreases slightly over almost the entire frequency range. The main resonance frequency stays at 0.6 kHz. Below
0.8 kHz, the amplitude decreases by 2.5 dB. Above 2.5 kHz, the amplitude decreases by up to 5 dB, with the
exception of a sharp dip at 6 kHz and an increase above 6 kHz.



370

Fig. 8 Simulated pressure gain of the chicken ME with normal outward TM (base model), completely flat TM, shallow TM (cone depth reduced by 50%), deep TM (cone depth increased by 50%) and inverted inward TM

4. Discussion

4.1 *The flexibility of the single-ossicle ear*

375 4.1.1 *The effect of flexibility on middle-ear sound conduction*

The flexibility of the extracolumella contributes to the motion of the columellar apparatus. At low frequencies, the extracolumella performs a rotating motion around an axis at the posterior rim of the TM, although the exact location of the fulcrum axis differs between studies and species. The rotating extracolumella would function as a second-class lever, increasing the force transmitted to the footplate. Rotations of the extracolumella are converted into piston-like motions of the columella and footplate (Muysshondt et al. 2018) due to bending of the intracolumellar connection as proposed by Pohlman (1921) for the chicken, or due to bending of the extracolumella itself as described by Manley (1990) for reptiles and birds in general. The present model showed that, at low frequencies, the flexible extracolumella indeed rotates around an axis at the posterior rim of the TM. This rotation is converted into a piston-like motion of the columellar shaft and footplate through bending in the extrastapedius, as explained by Manley (1990). The amplitude ratio of 2.7 between umbo and footplate was in the range of 2–3 as typically observed for the ratio in birds and reptiles (Rosowski 2013). When extracolumella

380

flexibility was artificially reduced, the columella and extracolumella vibrated as one combined structure. The columellar apparatus showed a mostly piston-like motion with a much smaller umbo-to-footplate ratio of 1.5. At low frequencies, the ME pressure gain (Fig. 5) and footplate motion (Fig. 7, upper panels) were larger in the flexible model than in the stiff model. This difference was due to the larger motion of the umbo in the flexible model, although the relative transfer of displacement from umbo to footplate was larger in the stiff model. An extracolumella that is too stiff thus constrains vibrations of the TM and umbo too much, although an extracolumella that is too flexible would fail to transfer vibrations further to the columella. This reasoning was also made by Funnell et al. (1993) to describe the flexibility of the manubrial process of the malleus in the cat.

Experimental studies suggest that the second-class lever model holds for frequencies below 1 kHz, but at higher frequencies the behavior deviates from this picture (e.g., Rosowski et al. 1985); the ratio of the lever (amplitude of input over output) was found to increase above 4 kHz in the tokay gecko (Manley 1972b), marbled velvet gecko (Werner et al. 1998) and pigeon (Gummer et al. 1989a), indicating a deterioration of sound transmission through the columellar apparatus. In pigeon, this observation was accompanied by an increasing phase lag between umbo and footplate. The present model showed that, in the mid-frequency range, the motion of the columellar apparatus started to deviate from a simple lever action (Fig. 7, mid panels); at 1 kHz, a second rotation of the extracolumella emerged on top of the original rotation in the flexible model, and a phase lag between umbo and footplate vibration arose. This change at 1 kHz was not observed in the stiff model. Therefore, the altered vibration modes of the columellar apparatus (e.g., Rosowski et al. 1985; Manley 1972b; Werner et al. 1998; Gummer et al. 1989a) can be partly explained by the flexibility of the extracolumella.

The effect of flexibility of the columellar apparatus on ME sound conduction was investigated by a simple model in Mason and Farr (2013). The model consisted of two masses (extracolumella and columella) connected together by a spring (intracolumellar connection or flexing part of the extracolumella); the second mass (columella) was supported by a second spring (annular ligament) in the skull. The model showed that flexibility generally reduces the conduction of sound through the system, especially at high frequencies. In the present model, it was found that vibrations of the flexible extracolumella were more complicated at high frequencies than at low and mid frequencies (Fig. 7, lower panels). The processes of the extracolumella showed complicated bending patterns, guiding TM motions as transverse traveling waves toward the columella; these motions were transmitted little beyond the point where the three processes of the extracolumella join together. This effect was not observed in the stiff model, which showed a much stronger coupling of the motions of the extracolumella to the columella. As a result, the footplate displacement (Fig. 7, lower panels) and ME pressure gain (Fig. 5) were

larger in the stiff model, although motions of the extracolumella were larger in the flexible model. These findings mostly agree with the explanation of Manley (1972a) that flexibility of the extracolumella is largely responsible for the poor high-frequency transmission and hearing of non-mammals. According to Manley (1972a), the impedance of the columella and/or IE experienced by the TM and extracolumella increases above a certain frequency, so the columella becomes more resistant to movement. As a result, the main process of the extracolumella (infrastapedius in lizards and extrastapedius in birds) bends between the umbo and the connection with the columella, which absorbs most of the vibration energy rather than transmitting it to the columella. The high-frequency bending patterns in the present study are, however, more complicated than what is presented in Manley (1972a,b). It is unclear if this difference is due to a lack of full-field data of extracolumella motion in Manley (1972b), who measured at the distal tip and at a point halfway down the central process of the extracolumella, or is a difference between species.

Although the present model explains how the flexibility of the extracolumella deteriorates sound conduction in the single-ossicle ME at frequencies up to 8 kHz, it does not teach us anything about why the mammalian three-ossicle chain is superior to the single-ossicle apparatus at even higher frequencies. One aspect that could explain the difference in high-frequency performance is the inertia of the ME chain. In mammals, the axis of rotation of the ossicular lever is located at the connection between the malleus and incus. In many cases, the mass of these ossicles is largely concentrated around this axis. Therefore, the rotational axis and the center of mass largely coincide, which reduces the moment of inertia and improves the high-frequency transmission (e.g., Fleischer 1978; Puria and Steele 2010). In non-mammals, the axis of rotation of the columellar lever lies at the edge of the TM. The columella and extracolumella are located at a considerable distance from this axis, so the moment of inertia is large and the high-frequency response is reduced (Norberg 1978; Saunders et al. 2000). In birds, the oblique orientation of the columellar apparatus with respect to the TM plane can help to bring its center of mass closer to the axis of rotation, which potentially reduces the moment of inertia. Other hypotheses have been proposed to explain the superior high-frequency performance of the three-ossicle chain, which describe alterations in the mode of motion of the ossicles at high frequencies (e.g., Fleischer 1978; Puria and Steele 2010). It has been put forward that the mammalian ME might act as a transmission line (e.g., Overstreet and Ruggero 2002). In this theory, the ME components are considered as a sequence of masses and springs that result in wideband and efficient sound transmission at high frequencies, but at the cost of acoustic delay. The predictions of this hypothesis were found to be valid in the range of 5–35 kHz in gerbil, but not at lower or higher frequencies (Ravicz et al. 2008). Possibly, the suspension system of the ME ligaments and the two ME

muscles play a role in the high-frequency performance of the mammalian ME, which are less pronounced in the ME of non-mammals (Rosowski 2013). Clearly, more experimental and modeling work on the high-frequency behavior in mammals and non-mammals is needed to find a conclusive answer.

450 4.1.2 *The function of flexibility*

Despite the fact that flexibility deteriorates the high-frequency performance of the single-ossicle ME, flexibility in the columellar apparatus may be important for other reasons. Mason and Farr (2013) reviewed the function of flexibility in the ME of different vertebrates. Their conclusion was that flexibility most likely serves to buffer the ME against high-amplitude quasi-static pressure changes, although in general flexibility reduces sound
455 conduction at high frequencies. In our previous static model of the chicken ME (Muyshondt et al. 2019), it was found that flexibility of the extracolumella buffers static displacements of the TM. Increasing the flexibility boosted the relative transfer of displacement from umbo to footplate, but reduced the TM displacement by the same amount. As a result, flexibility had almost no effect on absolute footplate displacements. Nevertheless, a stiff extracolumella may increase the stress in the TM under static pressure, which could make rupture of the
460 membrane more likely or reduce sound conduction when the ME is exposed to a quasi-static pressure.

Flexibility may be important to protect the ME from structural damage (Manley 1990). In lizards, the ear canal is very short or completely absent, and the ME is widely exposed to the mouth cavity. In birds, the ME is more isolated from the body surface and the inside of the skull, although birds still have shorter ear canals than mammals and ME cavities that communicate with air spaces in the skull. Manley (1990) noted that the
465 extracolumella is more flexible in the widely exposed ME of lizards than in the ME of birds. This increased flexibility in lizards may be needed to minimize the risk of ME damage by external or internal disturbances. For example, a flexible extracolumella could help to protect the bony columella from injury when the lizard is chewing or swallowing, which can go along with very strong head movements. These ideas could also hold to a lesser degree for birds.

470 Although the present study showed that the flexibility of the columellar apparatus leads to a reduction in sound conduction at high frequencies, it improved sound conduction at low frequencies due to a reduction in the TM constraint. It thus seems that flexibility of the extracolumella serves to enhance the transmission at low frequencies by minimizing the TM constraint, rather than to enable piston-like motion of the footplate by bending of the extrastapedius (Manley 1990), as a piston-like motion was also obtained with a stiff columellar
475 apparatus. Interestingly, it was found that chickens are able to detect infrasound with frequencies down to 9.1 Hz

(Hill et al. 2014). The pigeon was shown to detect infrasound down to 10 Hz (Kreithen and Quine 1979), and the guinea fowl even displayed cochlear responses down to 5 Hz (Theurich et al. 1984). The ability to detect infrasound may thus be widespread among birds. In this sense, it could be possible that the flexible avian columellar apparatus is better adapted to very low frequencies compared to the human three-ossicle chain, where the TM is coupled to a stiff manubrium.

4.2 *The shape of the tympanic-membrane cone*

4.2.1 *The effect of conical shape in the literature*

The effect of the inward TM cone shape in mammals was investigated by FE models of the mammalian ME. Funnell and Laszlo (1978) investigated the effect of TM cone depth and curvature on linear static displacements of the TM and manubrium in the cat. It was found that increasing TM curvature decreases the peak displacement in the membrane's body, but increases the umbo displacement; i.e., a curved TM couples membrane vibrations better to the malleus. This behavior was explained by the effect of hoop stiffness: a non-curved shell cannot use its in-plane stiffness but only its low bending stiffness to resist transverse loads when the shell is thin; as a result, the impedance of the TM becomes small compared to the ossicular load, so pressures on the TM are more easily handled by deforming the membrane than by displacing the manubrium. Increasing the depth of the TM cone in the neighborhood of the actual anatomical depth decreased the umbo and manubrial displacement, which was attributed to an increase in TM stiffness with increasing cone depth. In the updated model of Funnell (1983), which studied the natural frequencies of the TM, it was noted that the TM curvature and depth are in the right zone to broaden the frequency response of the TM as much as possible.

Koike et al. (2001) investigated the effect of TM cone depth on TM vibrations and the ME pressure gain in a model of the human ME. Similarly to the calculations of manubrial displacement by Funnell and Laszlo (1978), they found that the ME pressure gain at low frequencies decreases with increasing cone depth in the neighborhood of the actual anatomical depth. At high frequencies, however, the resonance frequency and pressure gain increases with increasing cone depth. When the TM was nearly flat, the pressure gain showed an overall decrease over the entire frequency range, especially at high frequencies. This difference in behavior was also attributed to a higher stiffness of the conical membrane. When the TM is nearly flat, its inward or outward displacement occurs in a direction perpendicular to the TM plane, so it is only impeded by the small bending stiffness of the thin TM. When the TM is conical, its inward and outward deflection also causes a partial in-plane deformation of the TM, which is impeded by the larger in-plane stiffness of the membrane. In theory, such in-

505 plane deformations also occur when the TM cone has no curvature; i.e., when radial cross sections of the TM cone are straight lines. As a result, the increased impedance of the conical TM better matches the high impedance of the malleus, so displacements of the TM are better coupled to the manubrium.

In Fay et al. (2006), the effect of TM cone depth was investigated on the ME pressure gain in a model of the cat ME. Their model considered the organized radial and circumferential fiber arrangement and layered structure
510 of the curved, conical TM. Similarly to Koike et al. (2001), they found that increasing the cone depth reduces the pressure gain at low frequencies, but increases the resonance frequency and pressure gain at high frequencies. Also in their model, a nearly flat TM reduced the response over the entire frequency range, especially at high frequencies. This result was attributed to the specific shape and mechanical properties of the TM. The toroidal outer portions of the membrane are relatively flexible and have a large surface area, which provides a low
515 impedance matched to the air in the ear canal. The steep inner conical portions contain many radial fibers that are stiff in the direction needed to drive the umbo, which provides a high impedance matched to the stiff manubrium. The TM smoothly transitions from low- to high-impedance vibrations between these two regions, thus maximizing the transmission of sound energy to the malleus. Following Funnell et al. (1987), it was noted that the frequency response was smoother close to the manubrium than away from it. This behavior at the
520 manubrium was attributed to a spatial integration over the TM due to the fact that the manubrium is stiff; the manubrium averages out the local variations in the TM's frequency response which originate from the multiple vibration modes of the TM. Fay et al. (2006) concluded that the conical shape of the TM plays a crucial role in the production of these multiple vibration modes, which are needed to deliver the smooth response and sensitivity at high frequencies.

525 4.2.2 *The effect of conical shape in the present study*

Similarly to the mammalian ME models (Koike et al. 2001; Fay et al. 2006), the present model of the chicken ME showed that the low-frequency pressure gain decreases with cone depth, while the resonance frequency and high-frequency pressure gain increase with cone depth, at least up to 2–4 kHz. Between 0.5 and 2 kHz, the boost of the pressure gain due to a 50% increase in cone depth was small compared to the loss of the pressure gain due
530 to a 50% decrease in cone depth. Therefore, the chicken ME would not much benefit from making the TM cone even deeper than it is.

When the TM was made completely flat, there was a strong decrease in the low- to mid-frequency pressure gain. An outward conical TM thus performed better than a flat TM. In contrast to the models of Koike et al.

(2001) and Fay et al. (2006), there was no clear decrease in the pressure gain above 2 kHz when the TM was made flat. This discrepancy between mammals and non-mammals could partially originate from a difference in flexibility of the ME components coupled to the TM. In mammals, the TM was better at coupling displacements to the stiff manubrium at high frequencies when it had an inward conical shape than when it was flat. In chicken, the difference in umbo motion between the models with outward conical TM and flat TM was not substantial above 2 kHz, as both models showed a similar coupling of TM displacements to the extracolumella. However, when the stiffness of the extracolumella was artificially increased, the umbo motion in the conical model increased relative to the flat model at high frequencies above 2 kHz (not shown). Therefore, it seems that the effect of TM cone shape at high frequencies increases as the adjoining ossicular components become stiffer. Nevertheless, the mentioned difference in high-frequency behavior between the chicken and mammalian models is probably also due to a difference in values used for the TM Young's modulus [2 MPa in the present study; 33.4 MPa in Koike (2001); ~ 100 MPa in Fay et al. (2006)], as an increase in the Young's modulus drives the frequency response of the system to higher frequencies.

When the outward cone of the TM was inverted to form an inward conical TM, the ME pressure gain decreased slightly over almost the entire frequency range. The single-ossicle ME thus performed slightly better when the TM bulged outwards than when it bulged inwards. This might be explained by the fact that the umbo motion and the transmission from umbo to footplate decreased when the TM was inverted (not shown). Why the umbo motion was smaller in the inward model is not fully clear. The transmission from umbo to footplate, on the other hand, was smaller in the inward model (umbo-to-footplate ratio of 3.5) than in the outward model (umbo-to-footplate ratio of 2.7) because of the deformed shape of the extracolumella. To create the inward TM cone shape, the extrastapedius was inclined relative to the columella, and also the configuration of the infra- and suprastapedius was changed (Fig. 3c). In the inward model, a flexing motion of the extracolumella occurred at the points where the extrastapedius and infrastapedius were bent to create the inward TM geometry, which led to a reduction in transmission from umbo to footplate (not shown). The reduced transmission can also be attributed to the modified configuration of the suprastapedius. In the present models, the distal end of the suprastapedius represents the rotation axis of the extracolumella. In the outward model, the suprastapedius forms a nearly 90° angle relative to the columella. As a result, the columella vibrates in a pure piston-like manner along the arc of a circle centered at the rotation axis of the extracolumella (Norberg 1978). In the inward model, the suprastapedius is deformed such that the angle between the columella and suprastapedius is no longer 90°, so the piston-like motion of the columella is hindered. Therefore, the transmission appears to be optimal when the suprastapedius

and columella form a right angle, while the extrastapedius and columella form a straight angle. This condition is only fulfilled in the outward model.

Instead of preserving the orientation of the columella and altering the inclination of the extrastapedius relative to the columella to create the inward TM geometry, there was also a possibility to retain the orientation of the extrastapedius relative to the columella and change the inclination of the entire columellar apparatus. This operation would minimize the deformation of the extracolumella, but it would change the natural position and orientation of the IE relative to the TM, leading to a nearly 90° angle between the oval window and TM base plane. Alternatively, the inclination of the extrastapedius and orientation of the IE can both be preserved if the side processes of the extracolumella (infra- and suprastapedius) are removed in the outward model before creating the inward model. However, these processes are important to enable the piston-like motion of the columella (von Békésy 1949). Thus, a straight angle between the columella and extrastapedius and a right angle between the columella and suprastapedius can only exist when the TM cone bulges outwards. This reasoning could partly explain why the single-ossicle ME of birds prefers the configuration of an outward conical TM over an inward conical TM.

4.3 *The effect of the inner-ear load*

Due to a lack of measurement data of the IE load in chicken, the load was estimated from measurements of the IE load in ostrich. The IE load was modeled as a mass-damper system, and a geometrical scaling was applied from the ostrich to the chicken. In birds, the effect of the IE load on the sound-induced vibration response of the footplate has only been measured in pigeon (Gummer et al. 1989b); draining the IE fluid increased the footplate vibration response by about 8 dB on average (Fig. 4a in Gummer et al. 1989b). In the present chicken model, the IE load affected the footplate vibration response above the resonance frequency by 7.5 dB on average (Fig. 4), so the order of magnitude of the IE load is realistic. The sensitivity analysis in the present model can be used to account for the uncertainty in the precise value of the IE load. Large variations of 50% in the IE load magnitude affected the ME pressure gain by less than 6 dB at low frequencies (Fig. 5), and the effect was mainly determined by resistance R (Fig. 6, upper panel); the effect decreased with frequency to less than 3 dB at mid and high frequencies (Fig. 5), where it was mainly determined by mass M (Fig. 6, lower panels).

5. Conclusion

A dynamic 3D FE model of the chicken ME was developed to investigate the effect of flexibility of the columellar apparatus and the conical shape of the TM on sound conduction through the single-ossicle ME

between 0.125 and 8 kHz. It was found that increasing the stiffness of the extracolumella in the columellar apparatus decreases the pressure gain of the ME at low frequencies, but increases the pressure gain at high frequencies. The increase at high frequencies could be attributed to an increase in coupling of displacements of the extracolumella to the columella. In the normal model with flexible extracolumella, vibrations of the extracolumella were interrupted close to the connection with the columella, as it poses a high impedance to the extracolumella. As a result, the conduction of sound to the columellar footplate was reduced. The decline in the transmission performance of the ME at high frequencies up to 8 kHz was in agreement with measurements of the vibration response in single-ossicle MEs of different non-mammals. The effect of TM cone shape was investigated by changing the depth and orientation of the outward TM cone. Similarly to the inward conical TM of mammals, it was found that the outward conical TM in chicken enhances ME sound conduction, as it delivers a higher pressure gain than a flat TM. When the cone shape of the TM was inverted to form an inward conical TM like in mammals, the ME pressure gain decreased slightly over the entire frequency range. This decrease originated from a reduced umbo motion and transmission from umbo to footplate, which was attributed to an increase in bending behavior of the extracolumella and a reduction in piston-like columella motion in the model with inward TM. Possibly, the single-ossicle ME in chicken prefers an outward over an inward conical TM as it preserves a straight angle between the columella and extrastapedius and a right angle between the columella and suprastapedius, which provides the optimal transmission.

610 **Acknowledgements**

We thank Dr. R. Claes and Dr. J. Goyens for their help with the micro-CT scanning. We acknowledge the funding agency, the Research Foundation–Flanders (FWO), for their financial support, Grant no. 11T9318N.

Compliance with ethical standards

Conflict of interest

615 The authors declare that they have no conflict of interest.

References

- Arechvo I, Zahnert T, Bornitz M, Neudert M, Lasurashvili N, Simkunaite-Rizgeliene R (2013) The ostrich middle ear for developing an ideal ossicular replacement prosthesis. *Eur Arch Otorhinolaryngol* 270:37–44. <https://doi.org/10.1007/s00405-011-1907-1>
- 620 Bergevin C, Olson ES (2014) External and middle ear sound pressure distribution and acoustic coupling to the tympanic membrane. *J Acoust Soc Am* 135:1294–1312. <https://doi.org/10.1121/1.4864475>

- De Greef D, Pires F, Dirckx JJJ (2017) Effects of model definitions and parameter values in finite element modeling of human middle ear mechanics. *Hear Res* 344:195–206. <https://doi.org/10.1016/j.heares.2016.11.011>
- 625 Fay JP, Puria S, Steele CR (2006) The discordant eardrum. *PNAS* 103:19743–19748. <https://doi.org/10.1073/pnas.0603898104>
- Filogamo G (1949) Recherches sur la structure de la membrane du tympan chez les differents vertebres. *Acta Anat* 7:248–272. <https://doi.org/10.1159/000140387>
- Fleischer G (1978) Evolutionary principles of the mammalian middle ear. *Adv Anat Embryol Cell Biol* 55:1–76. https://doi.org/10.1007/978-3-642-67143-2_1
- 630 Funnell WRJ (1983) On the undamped natural frequencies and mode shapes of a finite-element model of the cat eardrum. *J Acoust Soc Am* 73, 1657–1661. <https://doi.org/10.1121/1.389386>
- Funnell WRJ, Laszlo CA (1978) Modeling of the cat eardrum as a thin shell using the finite-element method. *J Acoust Soc Am* 63:1461–1467. <https://doi.org/10.1121/1.381892>
- Funnell WRJ, Decraemer WF, Khanna SM (1987) On the damped frequency response of a finite-element model of the cat eardrum. *J Acoust Soc Am* 81:1851–1859. <https://doi.org/10.1121/1.394749>
- 635 Funnell WRJ, Khanna SM, Decraemer WF (1993) On the degree of rigidity of the manubrium in a finite-element model of the cat eardrum. *J Acoust Soc Am* 91:2082–2090. <https://doi.org/10.1121/1.403694>
- Gan RZ, Feng B, Sun Q (2004) Three-dimensional finite element modeling of the human ear for sound transmission. *Ann Biomed Eng* 32:847–859. <https://doi.org/10.1023/B:ABME.0000030260.22737.53>
- 640 Gummer AW, Smolders JWT, Klinke R (1989a) Mechanics of a single-ossicle ear: I. The extra-stapedius of the pigeon. *Hear Res* 39:1–14. [https://doi.org/10.1016/0378-5955\(89\)90077-4](https://doi.org/10.1016/0378-5955(89)90077-4)
- Gummer AW, Smolders JWT, Klinke R (1989b). Mechanics of a single-ossicle ear: II. The columella footplate of the pigeon. *Hear Res* 39:15-25. [https://doi.org/10.1016/0378-5955\(89\)90078-6](https://doi.org/10.1016/0378-5955(89)90078-6)
- Hemilä S, Nummela S, Reuter T (1995) What middle ear parameters tell about impedance matching and high frequency hearing. *Hear Res* 85:31–44. [https://doi.org/10.1016/0378-5955\(95\)00031-x](https://doi.org/10.1016/0378-5955(95)00031-x)
- 645 Hill EM, Koay G, Heffner RS, Heffner HE (2014) Audiogram of the chicken (*Gallus gallus domesticus*) from 2 Hz to 9 kHz. *J Comp Physiol A* 200:863–870. <https://doi.org/10.1007/s00359-014-0929-8>
- Jiang S, Gan RZ (2018) Dynamic properties of the human incudostapedial joint – Experimental measurement and finite element modeling. *Med Eng Phys* 54:14–21. <https://doi.org/10.1016/j.medengphy.2018.02.006>
- 650 Kinsler LE, Frey AR, Coppens AB, Sanders JV (1999) Fundamentals of acoustics. Wiley, New York
- Kirikae J (1960) The structure and function of the middle ear. Dissertation, University of Tokyo
- Koike T, Wada H, Kobayashi T (2001) Effect of depth of conical-shaped tympanic membrane on middle-ear sound transmission. *JSME Int J Ser C* 44:1097–1102. <https://doi.org/10.1299/jsmec.44.1097>
- Kreithen ML, Quine DB (1979) Infrasound detection by the homing pigeon: a behavioral audiogram. *J Comp Physiol A* 129:1–4. <https://doi.org/10.1007/BF00679906>
- 655

- Larsen ON, Christensen-Dalsgaard J, Jensen KK (2016) Role of intracranial cavities in avian directional hearing. *Biol Cybern* 110:319–331. <https://doi.org/10.1007/s00422-016-0688-4>
- Maftoon N, Funnell WRJ, Daniel SJ, Decraemer WF (2015) Finite-element modelling of the response of the gerbil middle ear to sound. *J Assoc Res Otolaryngol* 16:547–567. <https://doi.org/10.1007/s10162-015-0531-y>
- 660 Manley GA (1972a) A review of some current concepts of the functional evolution of the ear in terrestrial vertebrates. *Evolution* 26:608–621. <https://doi.org/10.2307/2407057>
- Manley (1972b) Frequency response of the middle ear of geckos. *J Comp Physiol* 81:251–258. <https://doi.org/10.1007/BF00693630>
- Manley GA (1990) Overview and outlook. In: Manley GA (ed) *Peripheral hearing mechanisms in reptiles and birds*. Zoophysiology. Springer, Berlin, pp 253–273. https://doi.org/10.1007/978-3-642-83615-2_14
- 665 Manley (2010) An evolutionary perspective on middle ears. *Hear Res* 263:3–8. <https://doi.org/10.1016/j.heares.2009.09.004>
- Manley GA, Sienknecht UJ (2013) The evolution and development of middle ears in land vertebrates. In: Puria S, Fay RR, Popper AN (eds) *The middle ear. Science, otosurgery, and technology*. Springer, New York, NY, pp 7–30. https://doi.org/10.1007/978-1-4614-6591-1_2
- 670 Mason MJ, Farr MRB (2013) Flexibility within the middle ears of vertebrates. *J Laryngol Otol* 127:2–14. <https://doi.org/10.1017/S0022215112002496>
- Mills R, Zhang J (2006) Applied comparative physiology of the avian middle ear: the effect of static pressure changes in columellar ears. *J Laryngol Otol* 120:1005–1007. <https://doi.org/10.1017/S0022215106002581>
- Motallebzadeh H, Maftoon N, Pitaro J, Funnell WRJ, Daniel SJ (2017) Finite-element modeling of the acoustic input admittance of the newborn ear canal and middle ear. *JARO* 18:25–48. <https://doi.org/10.1007/s10162-016-0587-3>
- 675 Muyshondt PGG, Aerts P, Dirckx JJJ (2016) Acoustic input impedance of the avian inner ear measured in ostrich (*Struthio camelus*). *Hear Res* 339:175–183. <https://doi.org/10.1016/j.heares.2016.07.009>
- Muyshondt PGG, Claes R, Aerts P, Dirckx JJJ (2018) Quasi-static and dynamic motions of the columellar footplate in ostrich (*Struthio camelus*) measured ex vivo. *Hear Res* 357:10–24. <https://doi.org/10.1016/j.heares.2017.11.005>
- 680 Muyshondt PGG, Aerts P, Dirckx JJJ (2019) The effect of single-ossicle ear flexibility and eardrum cone orientation on quasi-static behavior of the chicken middle ear. *Hear Res* 378:13–22. <https://doi.org/10.1016/j.heares.2018.10.011>
- Norberg RÅ (1978) Skull asymmetry, ear structure and function, and auditory localization in Tengmalm's owl, *Aegolius funereus* (Linné). *Phil Trans R Soc B* 282:325–410. <https://doi.org/10.1098/rstb.1978.0014>
- Overstreet EH, Ruggero MA (2002) Development of wide-band middle ear transmission in the Mongolian gerbil. *J Acoust Soc Am* 111:261–270. <https://doi.org/10.1121/1.1420382>
- 685 Pohlman AG (1921) The position and functional interpretation of the elastic ligaments in the middle-ear of *Gallus*. *J Morphol* 35:228–262. <https://doi.org/10.1002/jmor.1050350106>
- Puria S, Steele C (2010) Tympanic-membrane and malleus-incus-complex co-adaptations for high-frequency hearing in mammals. *Hear Res* 263:183–190. <https://doi.org/10.1016/j.heares.2009.10.013>

- 690 Ravicz ME, Cooper NP, Rosowski JJ (2008) Gerbil middle-ear sound transmission from 100 Hz to 60 kHz. *J Acoust Soc Am* 124:363–380. <https://doi.org/10.1121/1.2932061>
- Rosowski JJ (2013) Comparative middle ear structure and function in vertebrates. In: Puria S, Fay RR, Popper AN (eds) *The middle ear: science, otosurgery, and technology*, springer handbook of auditory research. Springer, New York, NY, pp 31–65. https://doi.org/10.1007/978-1-4614-6591-1_3
- 695 Rosowski JJ, Peake WT, Lynch TJ, Leong R, Weis TF (1985) A model for signal transmission in an ear having hair cells with free-standing stereocilia. II. Macromechanical stage. *Hear Res* 20:139–155. [https://doi.org/10.1016/0378-5955\(85\)90165-0](https://doi.org/10.1016/0378-5955(85)90165-0)
- Saunders JC, Duncan RK, Doan DE, Werner YL (2000) The middle ear of reptiles and birds. In: Dooling RJ, Fay RR, Popper AH (eds) *Comparative hearing: birds and reptiles*. Springer, New York, NY, pp 13–69. https://doi.org/10.1007/978-1-4612-1182-2_2
- 700 Smith G (1904) The middle ear and columella of birds. *Q J Microsc Sci* 48:11–22
- Starck JM (1995) Comparative anatomy of the external and middle ear of palaeognathous birds. *Adv Anat Embryol Cell Biol* 131:1–137. <https://doi.org/10.1007/978-3-642-79592-3>
- Theurich M, Langner G, Scheich H (1984) Infrasound responses in the midbrain of the guinea fowl. *Neurosci Lett* 49:81–86. [https://doi.org/10.1016/0304-3940\(84\)90140-X](https://doi.org/10.1016/0304-3940(84)90140-X)
- 705 Van der Jeught S, Dirckx JJJ, Aerts JRM, Bradu A, Podoleanu AG, Buytaert JAN (2013) Full-field thickness distribution of human tympanic membrane obtained with optical coherence tomography. *J Assoc Res Otolaryngol* 14:483–493. <https://doi.org/10.1007/s10162-013-0394-z>
- von Békésy G (1949) The structure of the middle ear and the hearing of one's own voice by bone conduction. *J Acoust Soc Am* 21:217–232. <https://doi.org/10.1121/1.1906501>
- 710 Werner YL, Montgomery LG, Safford SD, Igić PG, Saunders JC (1998) How body size affects middle-ear structure and function and auditory sensitivity in gekkonoid lizards. *J Exp Biol* 201:487–502
- Zhang X, Gan RZ (2013) Dynamic properties of human tympanic membrane based on frequency-temperature superposition. *Ann Biomed Eng* 41:205–214. <https://doi.org/10.1007/s10439-012-0624-2>
- 715 Zhang X, Gan RZ (2014) Dynamic properties of human stapedial annular ligament measured with frequency-temperature superposition. *J Biomech Eng* 136:0810041–0810047. <https://doi.org/10.1115/1.4027668>